Talanta 82 (2010) 367–371

Contents lists available at ScienceDirect

Talanta

journal homepage: www.elsevier.com/locate/talanta

Amine-terminated organosilica nanosphere functionalized prussian blue for the electrochemical detection of glucose

Wenjuan Li, Ruo Yuan*, Yaqin Chai

Chongqing Key Laboratory of Analytical Chemistry, College of Chemistry and Chemical Engineering, Southwest University, Chongqing 400715, China

ARTICLE INFO

Article history:
Received 31 December 2009
Received in revised form 19 April 2010
Accepted 25 April 2010
Available online 23 May 2010

Keywords:
Organosilica nanosphere functionalized prussian blue
Positively charged gold nanoparticles
Glucose oxidase
Biosensor

ABSTRACT

A new glucose biosensor had been developed by immobilizing positively charged gold nanoparticles (PGNs) on organosilica nanosphere functionalized prussian blue (OSiFPB)-modified gold electrode. The OSiFPB compound could not only effectively prevent the leakage of the PB mediator during measurements, but also easily form stable film on the electrode surface with efficient redox-activity and excellent conductivity. Furthermore, with the negatively charged surface of OSiFPB, this film could be used as an interface to adsorb the PGNs, which provided a congenial microenvironment for adsorbing biomolecules and decreased the electron-transfer impedance. So, with glucose oxidase as a model biomolecular, the proposed sensor showed rapid and highly sensitive amperometric response to glucose and this immobilization approach effectively improved the stability of the electron-transfer mediator. This work would be promising for construction of biosensor and bioelectronic devices.

1. Introduction

To improve the electron-transfer kinetics between enzyme and the electrode, many redox mediators, such as a series of soluble organic dyes [1–5], ferrocene and its derivatives [6], the prussian blue (ferric hexacyanoferrate) family [7], etc., have been introduced to the enzyme-based system. However, leakage has been a main problem for the entrapment of mediators due to their low molecular weight. To circumvent this problem, the monomeric mediators are usually linked directly with the organic polymer or proteins system in a number of reported literatures [8,9].

Silica-based organic–inorganic composites are attractive materials because they combine the both properties of the three-dimensional rigid porous silica and the organic component [10]. Moreover, they can provide suitable environment for the retainment of biomolecule activity. Yang et al. demonstrated a simple approach for an efficient entrapment of enzyme into silica matrix with retained bioactivity [11]. Yao et al. reported H_2O_2 biosensor by thionine-doped silica composite as a mediator [12]. Herein, we adopted a facile and bottom-up method to synthesize organosilica nanospheres, basing on synergic grafting polymerization, sol–gel reaction and amphiphilic self-assembly, i.e. the organosilica nanospheres was formed by hydrolysis and condensation of an alkyloxosilane-3-(trimethoxysilyl)propyl methacrylate (TMSPM) that was simultaneously polymerized using chitosan/*tert*-butyl hydroperoxide (TBHP) as redox-pair initiator [13]. Then PB was prepared in organosilica nanospheres suspension, which is donated as amine-terminated organosilica nanosphere functionalized prussian blue (OSiFPB). The OSiFPB might be greatly applied in a broad variety of bioelectronic or biosensing applications as it combined the following facts: (i) because of PBs rapid catalytic rate toward reduction of hydrogen peroxide (H_2O_2), it has been regarded as "artificial peroxidase", and widely used in the oxidase-based amperometric biosensors as an electron-transfer mediator; (ii) PB allows cathodic detection of H_2O_2 at a very low potential (0 to −0.1 V) and thus greatly enhances the immunity against the interference from the coexisting substances such as ascorbic acid, acetaminophen, and uric acid during blood sugar testing, (iii) the prepared OSiFPB overcomes the defect of PB mediator leakage due to the increase of the molecular weight of mediators and provided a remarkable synergistic augmentation to facilitate the electron-transfer process, which resulted in good stability and high sensitivity for the detection of analyte.

On the other hand, gold nanoparticle (nano-Au) is a kind of well known bio-nanomaterials for proteins immobilizing to fabricate electrochemical sensor [14–16]. Among them, the nano-Au played an important role. Firstly, as the merit of nano-Au with the high electrical conductivity, it can enhance the sensitivity of the sensor. Secondly, it provides more binding sites and more congenial microenvironment for biomolecules immobilization to retain the bioactivity of the enzyme, which can prolong the life of biosensor [17,18]. Generally, the nano-Au with negatively charged were the most commonly used. In fact, the positively charged gold nanoparticle (PGNs) can be at relatively high concentrations with

* Corresponding author. Tel.: +86 23 68252277; fax: +86 23 68254000.
E-mail address: yuanruo@swu.edu.cn (R. Yuan).

0039-9140/$ – see front matter © 2010 Elsevier B.V. All rights reserved.
doi:10.1016/j.talanta.2010.04.051

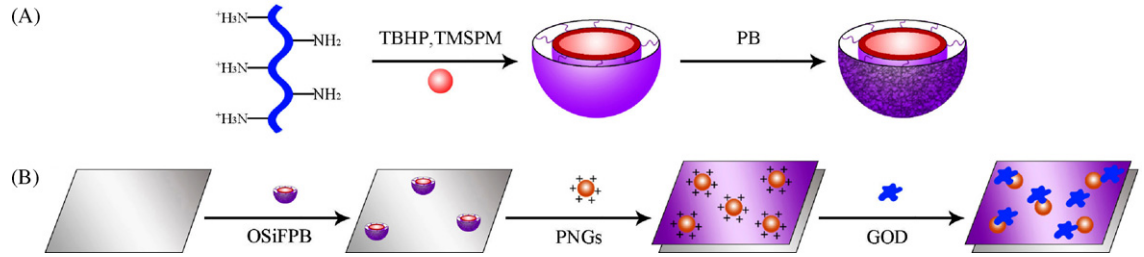

Fig. 1. Synthetic scheme for the preparation of the OSiFPB (A); illustration of the preparation process of modified electrode (B).

predefined size and shape, and with improved monodispersity and larger specific surface areas [19], which had been synthesized by Caruso's group. In our group, we have developed some biosensors, which were based on PGNs as templates to merge biomolecules [20,21].

Based on the above observations and our previous work, in the present paper, we report the construction of glucose biosensor using the OSiFPB and PGNs as building block. Details of the preparation, characterization of the synthesized OSiFPB and the electrochemical properties of biosensor are described in Section 2.

2. Experimental

2.1. Chemicals

Glucose oxidase (GOD), chitosan, 3-(trimethoxysilyl) propyl methacrylate (TMSPM), *tert*-butyl hydroperoxide (TBHP, 70% solution in water), 4-dimethylaminopyridine, tetraoctylammonium bromide, glucose, $NaBH_4$ and gold chloride were obtained from Sigma Chemical Co. (St. Louis, MO, USA). Acetic acid and hydrogen peroxide (30% solution) were obtained from Chemical Reagent Co., Chongqing, China. Phosphate buffered saline (PBS) solutions with different pH values were prepared with stock standard solutions of 0.025 M KH_2PO_4 and 0.025 M Na_2HPO_4. The supporting electrolyte was 0.1 M KCl. Twice-distilled water was used throughout. GOD stock solutions (2 mg/mL) were prepared with 0.1 M pH 6.5 PBS. PGNs with mean size of 10 ± 1.8 nm were prepared according to literature [19].

2.2. Apparatus and measurements

Amperometric experiments and cyclic voltammetric experiments were performed on a CHI 660A electrochemical work station (Shanghai CH Instruments Co., China) with a conventional three electrode system consisted of a modified gold electrode as working electrode, a platinum wire as auxiliary electrode, and a saturated calomel electrode (SCE) as reference electrode. All potentials were measured and reported versus the SCE. Transmission electron microscopy (TEM) was carried out on a TECNAI 10 (PHILIPS FEI Co., Holland). X-ray photoelectron spectroscopy (XPS) measurements were carried out using a VG Scientific ESCALAB 250 spectrometer, using Al Ka X-ray (1486.6 eV) as the light source. All the electrochemical experiments were carried out at room temperature.

2.3. Synthesis of organosilica nanosphere functionalized prussian blue (OSiFPB)

An OSiFPB composite was achieved as follows: firstly, the organosilica nanospheres were prepared according to the literature [13]. Briefly, in a flask equipped with a condenser, 100 mL of chitosan solution (0.5 wt%) containing acetic acid (0.6 wt%) was vigorous stirred for 30 min with nitrogen atmosphere. Then, about 2 mL TMSPM monomer was added dropwise at 80 °C and stirred for 5 min. Following that, 1 mL of TBHP (20 mM) aqueous solution was added in one time with constant stirring. After being stirred further for 4 h under nitrogen, stable latex was obtained. The resultant nanospheres were carefully washed and purified with 0.6% acetic acid by repeated centrifugation. Secondly, 4 mL of a 0.025 mol/L $K_3[Fe(CN)_6]$ solution was slowly dropped into 16 mL of the above solution containing 6.25 mmol/L $FeCl_2{\cdot}4H_2O$ under vigorous stirring at room temperature. In the process of mixing, the corresponding solution gradually turned dark blue. And then centrifugation was conducted by 0.6% HAc and water for at least three times, which is the obtained OSiFPB composite (as shown in Fig. 1(A)).

2.4. Preparation of the modified electrode

Before each modification, the gold electrode (AuE, $\Phi = 4$ mm) was polished with 0.3 and 0.05 mm alumina to obtain mirror-like surface. Then it was rinsed with distilled water and put in freshly prepared 3:7 mixtures of 30% hydrogen peroxide and concentrated sulfuric acid for 10 min and then rinsed thoroughly with water, followed by cleaning with acetone and twice-distilled water in an ultrasonic bath, respectively. Subsequently, 8 μL of OSiFPB suspension was cast onto the pretreated AuE surface and dried in air. Then, PGNs were dropped on the resulting electrode surface and allowed to dry at 4 °C. Finally, the electrode was immersed in 2 mg/mL GOD solution overnight to attach enzyme molecules to the electrode surface, which was denoted here as GOD/PGNs/OSiFPB/AuE. The preparation process of the biosensor was shown in Fig. 1(B).

3. Results and discussion

3.1. Characterizations of the OSiFPB by XPS and TEM

In order to confirm the adsorption of PB onto the surface of organosilica nanosphere, TEM experiments of organosilica nanosphere and OSiFPB were performed. The TEM image of the nanosphere is found in Fig. 2a and the sphere size was distributed in 50–90 nm with mean sizes around 80 nm. After modification with PB (Fig. 2b), the size became larger and the average diameter was about 100 nm. This appearance showed that the nanospheres were surrounded tightly by PB to form OSiFPB, indicating PB can be bound onto the organosilica nanosphere by virtue of the electrostatic attraction between the amino group of nanosphere surface and negatively charged PB.

To analyze the chemical composition in the OSiFPB compound, XPS characterization was employed. And the corresponding XPS survey spectrums from chitosan (a), organosilica nanosphere (b), OSiFPB (c) were displayed in Fig. 3, respectively.

As shown in Fig. 3a, there were intense O 1s signal, C 1s signal, N 1s signal characteristic, which should attribute to the respective atoms in chitosan. However, the Si 2p photoelectrons signal was detected in Fig. 3b, indicating that the formation of organosilica nanosphere. In Fig. 3c, as expected, Fe 2p peaks with

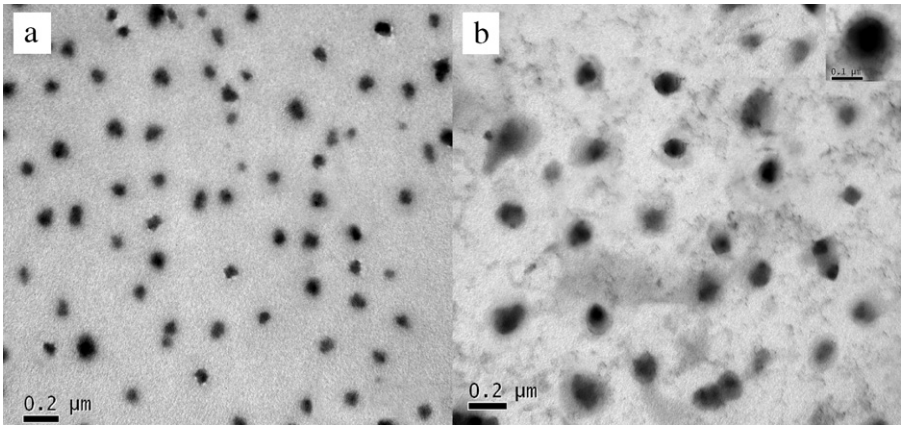

Fig. 2. TEM photos of organosilica nanosphere (a) and OSiFPB film (b).

binding energies of 707.7 eV for $2p_{3/2}$ and 720.7 eV for $2p_{1/2}$ can be clearly observed at the OSiFPB nanocomposites, which provided an evidence for the existence of Fe 2p peaks at the OSiFPB nanocomposites. Thus, these results can confirm the formation of organosilica nanosphere functionalized PB nanoparticles.

3.2. Electrochemical characteristics of the modified electrode

The cyclic voltammograms (CVs) of the biosensor, namely GOD/PGNs/OSiFPB/AuE electrode, present a pair of well defined redox peaks in PBS (pH 6.0) at different scan rates, as shown in Fig. 4.

The anodic peak potential (E_{pa}) and cathodic peak potential (E_{pc}) are located at 0.22 and 0.13 V, at scan rate of 50 mV/s, respectively. The separation of peak potentials (ΔE_p) is ca. 90 mV and the cathodic and anodic peak currents were of similar magnitude, with an I_{pa}/I_{pc} ratio of about unity. The formal potential ($E^{0'}$) calculated by averaging cathodic and anodic peak potentials, is ca. 0.18 V, which can be concluded that the peaks represented characteristics of redox couple of PB in OSiFPB, indicating the efficient redox-activity and excellent conductivity of OSiFPB film. As shown in inset A of Fig. 4, a linear relationship of peak current to the square root of scan rate was revealed in the scan rate range of 10–100 mV/s, showing a diffusion-controlled process. This result indicated that local cation concentration gradient may be developed during the electrochemical reaction, and the diffusion of cations from the solution to the electrode surface was the rate-limited step at the scan rates less than 100 mV/s. At higher sweep rates, the peak currents became proportional to scan rate (inset of Fig. 4B), which indicated that the reaction is a surface-controlled process. In addition, according to the model of Laviron equation [22], the apparent surface electron-transfer rate constant (k_s) can be estimated as 2.35 s^{-1}. The above results also show that the integration of OSiFPB and PGNs can provide a remarkable synergistic augmentation of sensor performance. The electroactive surface area (A) of GOD/PGNs/OSiFPB/AuE electrode was estimated to be 0.2456 cm^2 according to the Randles–Sevcik equation [23]. The high active surface area suggests that the OSiFPB and PGNs composite films provides a biocompatible microenvironment and favors an increased loading of the bioactive enzyme.

3.3. Effect of the value of pH on the response current

Investigation of the pH value of the detection solution on the performance of the biosensor is of great importance, because the activity of the immobilized GOD and the stability of PB are pH dependent. Fig. 5 shows the effect of pH in a series of PBS with the pH from 4.0 to 9.0 under constant glucose concentration (20.0 μM).

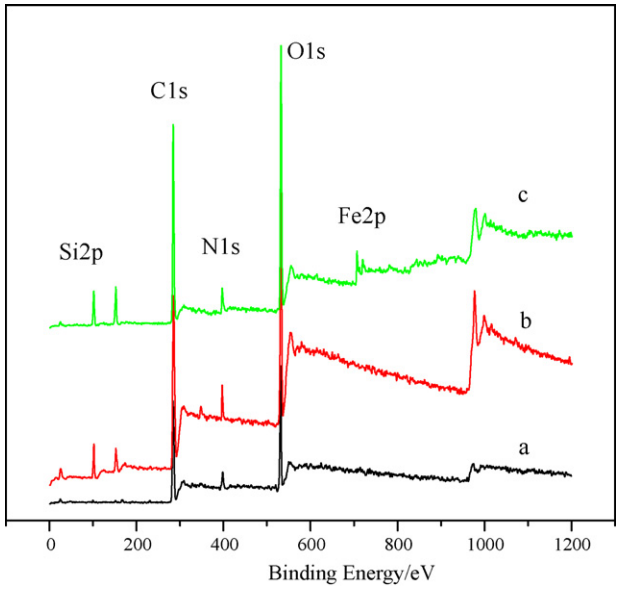

Fig. 3. The XPS spectra of chitosan (a), organosilica nanosphere (b) and OSiFPB (c).

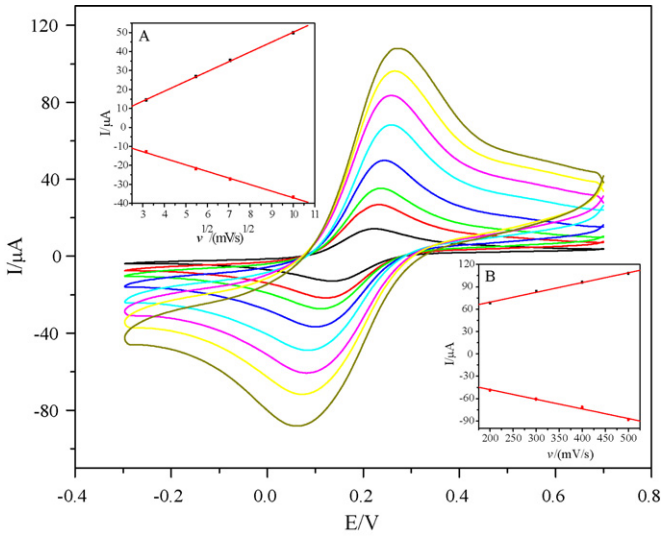

Fig. 4. CVs of GOD/PGNs/OSiFPB/AuE electrode in 0.025 M PBS (pH 6.0) at scan rate of (from inner to outer): 10, 30, 50, 100, 200, 300, 400 and 500 mV/s. Inset A: plot of I_p vs. $v^{1/2}$. Inset B: I_p vs. v.

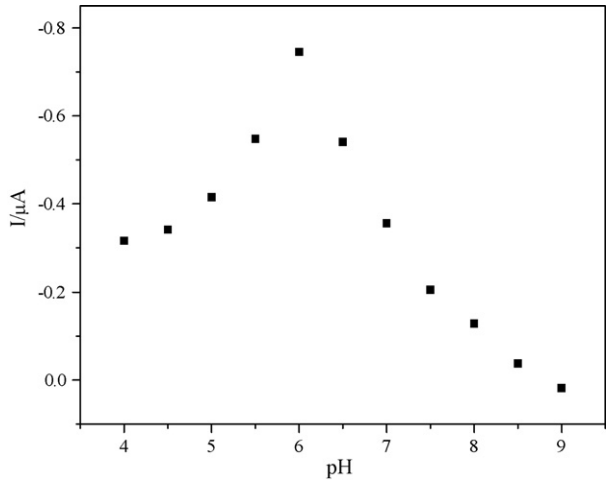

Fig. 5. Dependence of the current response of GOD/PGNs/OSiFPB/AuE electrode to 2.0×10^{-5} M glucose on the pHs of buffer solutions at an applied potential of −100 mV in 0.025 M PBS (pH 6.0).

With the increasing pH from 4.0 to 6.0 the response current increased, and the further increasing pH from 6.0 to 9.0 led to great decrease of the response current, producing an optimal pH value, that is pH 6.0 for the detection of glucose.

3.4. Cyclic voltammetric response of biosensor to glucose

The catalytic activity of the biosensor toward glucose was investigated by cyclic voltammetric measurements. Fig. 6 shows the CVs obtained with the biosensor in 0.025 M PBS (pH 6.0) without glucose (a) and with 1.2 mM glucose (b), respectively.

In the absence of glucose, the modified electrode gives no response and only the electrochemical behavior of OSiFPB was observed (Fig. 6a). With the addition of glucose, the CVs changed dramatically with a sharp increase in reduction peak current and a concomitant decrease in the oxidation peak current (Fig. 6b). It indicated that a catalytic reaction occurred on this biosensor. On the basis of measuring the electrocatalytic reduction current of H_2O_2 produced from the reaction of glucose and oxygen under the catalysis of GOD, the detection of glucose is achieved. The typical mechanism of the catalytic system based on the biosensor for

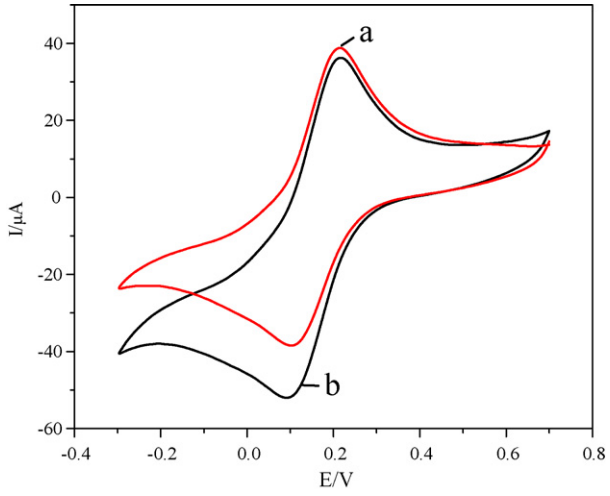

Fig. 6. CVs of the proposed electrode in 0.025 M PBS (pH 6.0) without glucose (a), with 1.2 mM glucose (b). Scan rate: 50 mV/s.

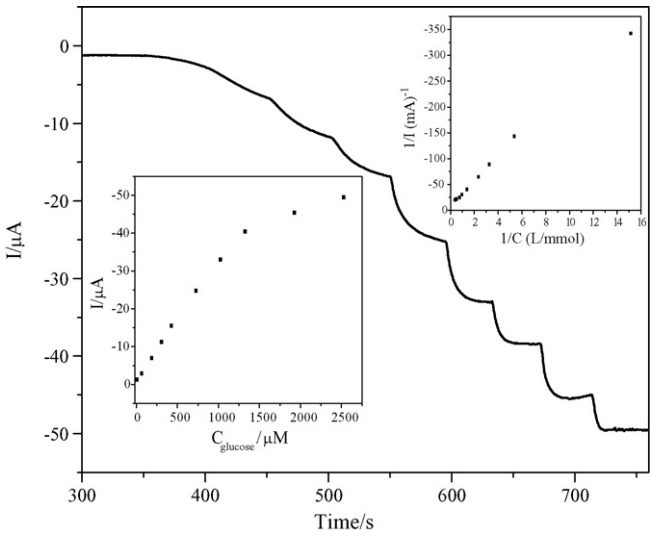

Fig. 7. Amperometric responses of the biosensor in stirred solutions to the successive additions of glucose. The lower inset shows linear calibration curves. The upper inset is the Lineweaver–Burk plot for measurement of the apparent Michaelis–Menten constant K_M^{app}.

detecting glucose can be described in the following scheme:

$$\text{GOD(FAD)} + \beta\text{-d-glucose} \rightarrow \text{GOD(FADH}_2\text{)} + \delta\text{-gluconolactone}$$

$$\text{GOD(FADH}_2\text{)} + O_2 \rightarrow \text{GOD(FAD)} + H_2O_2$$

$$K_2Fe^{2+}Fe^{2+}(CN)_6(\text{Prussian white}) \overset{H_2O_2}{\underset{e}{\rightleftharpoons}} (\text{Prussian blue})KFe^{3+}Fe^{2+}(CN)_6 + K^+$$

3.5. Response of the biosensor to glucose

We used the steady-state current to plot with the concentration of glucose. Fig. 7 showed the typical current–time response of the biosensor on successive step changes of glucose concentration under the optimized experimental conditions.

With the increase of the concentration of glucose, the biosensor responded rapidly. The lower inset of Fig. 7 displays the calibration curve of the biosensor for glucose determination. The response current increased linearly with the glucose concentration in the range of 6.0×10^{-6} to 1.3×10^{-3} M with a correlation coefficient of 0.997. From the slope of calibration curve, the detection limit of 2.0×10^{-6} M was estimated at signal-to-noise ration of three. The sensitivity for glucose determination was about 122.6 μA mM^{-1} cm^{-2}. The apparent Michaelis–Menten constant (K_M^{app}) is generally used to evaluate the biological activity of GOD (the upper inset of Fig. 7). According to Lineweaver–Burk equation [24], the value of K_M^{app} was estimated to be 1.8 mM, which indicated that the immobilized GOD possesses higher enzymatic activity and the GOD/PGNs/OSiFPB/AuE exhibits a higher affinity for glucose.

In addition, the analytical performance of the developed glucose biosensor has been compared with those of other glucose biosensors reported in the literatures [5,25–30]. Characteristics such as range of linearity of the corresponding calibration graph, sensitivity, limit of detection and K_M^{app} achieved are summarized for all of them in Table 1. As can be seen, the sensitivity achieved here is higher than those in most of works, the detection limit was lower, and the value of K_M^{app} was also better. The reasons might be the fact: on the one hand, we integrated the good biocompatibility of OSiFPB and the good conductivity of PGNs together, which could be favor for the electron transfer and enhances the sensitivity. On the other hand, the matrix might provide a more congenial microenvironment to maintain the intrinsic properties of enzyme, which could improve the affinity to glucose.

Table 1
Analytical properties of different glucose electrochemical biosensors.

Biosensor fabrication	Linear range (mM)	DL (μM)	Sensitivity (μA mM^{-1} cm^{-2})	K_M^{app} (mM)	Ref
GOx/PPy/CuHCNFe/GC	0.02–1.0	5.4	34.9	–	[25]
GOD/CS-PB/CS/AuE	0.002–0.4	0.397	–	3.73	[26]
GOD/CD-Fc/GNPs/Pt	0.08–11.5	15	18.2	6.42	[27]
GOD/MWNTs-Fc/CS/GC	0.0012–3.8	3.0	25	3.12	[28]
GOD/POAP/PB/Pt	–4	10	24	10.5	[29]
PTBO-GOD/CNT/GC	1–7	–	14.5	–	[5]
GOD/PB/Fe_3O_4/CPE	0.0005–0.8	0.1	–	0.0144	[30]
GOD/PGNs/OSiFPB/AuE	0.006–1.3	2.0	122.6	1.8	This work

3.6. Reproducibility of measurements and stability of biosensor

The reproducibility of the glucose biosensor was also investigated by detecting 20 μM glucose successively for six times, the relative standard deviation was 4.2%, demonstrating the biosensor has a good reproducibility. Additional experiments were carried out to test the stability over a period of 3 weeks. When not in use, the electrode was suspended above 0.1 M PBS at 4 °C in a refrigerator. The response to 0.1 mM glucose was tested every 2–3 days. The enzyme electrode retained 84.6% of its original response after over 3 weeks. This good stability maybe ascribed to the facts that the OSiFPB composite film could effectively prevent the leakage of the PB and the PGNs membrane could provide a good biocompatible microenvironment for the immobilization of GOD molecules.

3.7. Interference determination

The selectivity of the present sensor was examined by studying the effects of foreign species (such as ascorbic acid, uric acid, L-cys and L-tyrosine) on the determination of 0.1 mM glucose. Measurements were carried out by the value of the current ratio which was calculated by reading the current of the proposed biosensor in an assay solution containing 0.1 mM glucose and a 0.2 mM interfering substance and comparing it with the current from the proposed biosensor in the same assay solution containing only 0.1 mM glucose. From the results, the relative response current changes were 1.08 for ascorbic acid, 0.98 for uric acid, 0.97 for L-cys and 1.04 for L-tyrosine. These results indicate that above five tested interferents could not cause interference significantly to the determination of glucose, suggesting that the cascade schemes takes place at much lower potentials (−0.1 V), and therefore, the selectivity of the device is improved considerably.

4. Conclusions

We had demonstrated herein a kind of composite materials, OSiFPB, which was obtained by two-step conjugate synthesis with efficient redox-activity and excellent conductivity. It effectively prevented the leakage of the PB mediator during measurements. In addition, the presence of PGNs provided a congenial microenvironment for adsorbed biomolecules and decreased the electron-transfer impedance.

Take advantage of the both of OSiFPB and PGNs, the proposed biosensor showed a broader linear range, lower detection limit, high sensitivity, and superior stability. This work provided a new avenue for the electrochemical investigation of enzyme immobilization.

Acknowledgements

This work was supported by the NNSF of China (20675064), the Ministry of Education of China (Project 708073), the Natural Science Foundation of Chongqing City (2009BA1003), High Technology Project Foundation of Southwest University (XSGX02) and the Postgraduate Science and Technology Innovation Fund of Southwest University (ky2009003), China.

References

[1] W. Cheng, J. Jiang, S.J. Dong, E.K. Wang, Chem. Commun. (2002) 1706.
[2] A.S. Santos, A.C. Pereira, N. Durán, L.T. Kubota, Electrochim. Acta 52 (2006) 215.
[3] P. Du, P. Wu, C.X. Cai, J. Electroanal. Chem. 624 (2008) 21.
[4] D.W. Yang, H.H. Liu, Biosens. Bioelectron. 25 (2009) 733.
[5] Y.L. Yao, K.K. Shiu, Electrochim. Acta 53 (2007) 278.
[6] N.J. Sun, L.H. Guan, Z.J. Shi, N.Q. Li, Z.N. Gu, Z.W. Zhu, Anal. Chem. 78 (2006) 6050.
[7] P.A. Fiorito, V.R. Gonçales, E.A. Ponzio, S.I. Coïrdoba de Torresi, Chem. Commun. (2005) 366.
[8] M.P. García Armada, J. Losada, I. Cuadrado, B. Alonso, B. González, E. Ramírez-Oliva, C.M. Casado, Sens. Actuators B 88 (2003) 190.
[9] V.B. Kandimalla, V.S. Tripathi, H. Ju, Biomaterials 27 (2006) 1167.
[10] A. Walcarius, D. Mandler, J.A. Cox, M. Collinson, O. Lev, J. Mater. Chem. 15 (2005) 3663.
[11] S. Yang, W.Z. Jia, Q.Y. Qian, Y.G. Zhou, X.H. Xia, Anal. Chem. 81 (2009) 3478.
[12] H. Yao, J.M. Hong, N. Li, S. Xu, J.J. Zhu, J. Nanosci. Nanotechnol. 9 (2009) 2421.
[13] B. Fei, H.F. Lu, J.H. Xin, Polymer 47 (2006) 947.
[14] B. Ipe, K. Yoosaf, K.G. Thomas, J. Am. Chem. Soc. 128 (2006) 1907.
[15] S.J. Guo, E.K. Wang, Anal. Chim. Acta 598 (2007) 181.
[16] F.N. Crespilho, M. Emilia Ghica, M. Florescu, F.C. Nart, O.N. Oliveira Jr., C.M.A. Brett, Electrochem. Commun. 8 (2006) 1665.
[17] M.J. Wang, L.Y. Wang, G. Wang, X.H. Ji, Y.B. Bai, T.J. Li, S.Y. Gong, J.H. Li, Biosens. Bioelectron. 19 (2004) 575.
[18] C.X. Lei, Y. Yang, H. Wang, G.L. Shen, R.Q. Yu, Anal. Chim. Acta 513 (2004) 379.
[19] D.I. Gittins, F. Caruso, Angew. Chem. Int. Ed. 16 (2001) 3001.
[20] L.Y. Zhang, R. Yuan, Y.Q. Chai, X.L. Li., Anal. Chim. Acta 596 (2007) 99.
[21] Y. Zhuo, P.X. Yuan, R. Yuan, Y.Q. Chai, C.L. Hong, Biomaterials 29 (2008) 1501.
[22] E. Laviron, J. Electroanal. Chem. 101 (1979) 19.
[23] A.J. Bard, L.R. Faulkner, Electrochemical Methods: Fundamentals and Applications, 2nd ed., Wiley, New York, 2001, p. 231.
[24] R.A. Kamin, G.S. Wilson, Anal. Chem. 52 (1980) 1198.
[25] P.A. Fiorito, C.M.A. Brett, S.I. Coïrdoba de Torresi, Talanta 69 (2006) 403.
[26] X.Y. Wang, H.F. Gu, F. Yin, Y.F. Tu, Biosens. Bioelectron. 24 (2009) 1527.
[27] M. Chen, G.W. Diao, Talanta 80 (2009) 815.
[28] J.D. Qiu, W.M. Zhou, J. Guo, R. Wang, R.P. Liang, Anal. Biochem. 385 (2009) 264.
[29] D.W. Pan, J.H. Chen, L.H. Nie, W.Y. Tao, S.Z. Yao, Anal. Biochem. 324 (2004) 115.
[30] J.P. Li, X.P. Wei, Y.H. Yuan, Sens. Actuators B 139 (2009) 400.